Electrochemical Micromachining of Hastelloy C276 by Different Electrolyte Solutions

Arabian Journal for Science and Engineering
https://doi.org/10.1007/s13369-020-05032-1

RESEARCH ARTICLE-MECHANICAL ENGINEERING

Electrochemical Micromachining of Hastelloy C276 by Different Electrolyte Solutions

Gowtham Kumarasamy[1] · Poovazhagan Lakshmanan[1] · Geethapriyan Thangamani[2]

Received: 6 March 2020 / Accepted: 9 June 2020

Abstract

Micro-electrochemical machining (μECM) is a non-traditional material removal technique developed to cut incredibly hard surfaces which are not easy to cut by any traditional methods. Hastelloy C276 is a nickel-based superalloy, and its applications include equipment components of chemical processing units, food processing units and pharmaceutical industries. Due to the work hardening tendency, machining of Hastelloy C276 by conventional manner becomes exceedingly difficult. μECM can be a possible alternative fabrication technology for machining Hastelloy C276 particularly in micro-domain. This work demonstrates the μECM (micro-hole making) behavior of Hastelloy C276 using NaCl, $NaNO_3$ and hybrid mixture (NaCl + $NaNO_3$ + citric acid) as electrolyte solutions. L9 statistical design of experiments was employed to reduce the number of experiment trials required. Taguchi grey relational approach was executed to determine the most favorable machining variables. Confirmation tests were performed, and the error percentage was calculated. Surface irregularities of the machined parts were systematically examined by 3D surface roughness tester. Experimental results revealed that all the output performances are highly dependent on the type of electrolyte used. Hybrid electrolytic combination produced better material removal rate, lower overcut, lower conicity and most circular holes. Scanning electron microscopy images were used to identify the best-, moderate- and poor-quality micro-holes.

Keywords Micro-electrochemical machining · Hastelloy C276 · Electrolytes · Material removal rate · Taguchi · Scanning electron microscopy

1 Introduction

Due to the extraordinary anti-corrosive properties, Hastelloy (Ni-based superalloy) is extensively used in chemical processing units, energy, petrochemical, environmental pollution & control and desulfurization industries [1]. Machining of Ni and its alloys becomes more difficult because of its exceptional strength and below normal heat conductivity at elevated temperature [2–5]. Machining of Ni alloys at a speed of 300 m/min produces high working temperature in the order of 1000 °C [6, 7]. Due to product miniaturization and development of new materials with extreme properties, there is a need for advanced machining technologies [8].

✉ Poovazhagan Lakshmanan
poovazhaganl@ssn.edu.in

1 Sri Sivasubramaniya Nadar (SSN) College of Engineering, Chennai, India

2 SRM Institute of Science and Technology, Chennai, India

Researchers are motivated by the properties of Ni-based alloys such as shape control and metallurgical constraints to do research work in micro-domain [9]. Machining of hard materials with conventional machining process leads to more uneven surfaces, larger heat influenced region and high thermal stress. Production of micro-holes is the basic machining operation required in micro-/meso-components [10]. The established machining technique for micro-drilling in Ni and its alloy is electrical discharge machining (EDM). The drawback with EDM process is that it produces hard recast layer on the machined surfaces [11–13]. With less amount of tool wear, micro-electrochemical machining (μECM) can be a suitable material removal process for machining Ni alloys in micro-domain. μECM has wider applications in turbine blades manufacturing, parts of high compression engine, warheads, electronic and mechanical industries [14, 15].

When the anode (workpiece) and a cathode (electrode) are immersed into the electrolyte solution and DC current is supplied, the material is eroded and flushed away from the anode surface by μECM process. The quantity of material removed

Published online: 05 November 2020

from the surface depends on applied current and machining gap [16]. It is necessary to investigate the influence of various machining factors to find the optimized machining conditions for performing micromachining on Hastelloy. In this study, NaCl, $NaNO_3$ and hybrid mixture (NaCl + $NaNO_3$ + citric acid) are used as electrolyte solutions for micromachining Hastelloy C276. Taguchi grey relational approach is applied to identify the optimum machining factors for superior material removal rate (MRR), better finishing quality and lower conicity.

2 Experiments and Methods

2.1 Material for Study

The material chosen for the experimentation is commercially available Hastelloy C276. Hastelloy C276 has high corrosive resistance property due to the combination of nickel–molybdenum–chromium and tungsten, so it has wider applications in very harsh environments. In nickel-based superalloy category, Hastelloy C276 is the widely accepted alloy for most of the engineering applications [17]. Chemical composition of Hastelloy C276 is listed in Table 1. Chemical composition is obtained as per standard laboratory test. Table 2 represents the physical and mechanical properties of Hastelloy C276.

2.2 Electrolyte Selection

Electrolyte is chosen based on the characteristics of the selected workpiece surface [18]. Removal of material on the specimen surface occurs due to the conduction of voltage from tool to the workpiece. To improve the machining precision, the electrolyte must have proper concentration. Passive and non-passive kinds of electrolyte solutions are investigated in μECM process. The oxidizing anion available in the passive electrolyte like sodium nitrate ($NaNO_3$) produces the inactive layer on the machined area and evolutes oxygen within the stray current region.

Good machining accuracy can be achieved by maintaining the proper machining gap and sufficient concentration of electrolyte. Some chemicals and gas blending are also added as additive elements with electrolyte solution to get good machining accuracy. For example, the inclusion of chemical elements akin to $NaHSO_4$ with the electrolyte solution improves the machining accuracy. The requirement of high voltage for obtaining the better MRR is reduced with the usage of pre-heated electrolyte solution in μECM process. Widely accepted electrolytes in μECM process are NaCl, $NaClO_3$ and $NaNO_3$ [19].

Water [20, 21] and citric acid [12] are reported as the harmless and eco-friendly electrolytes that have very good machining efficiency. Micro-holes with higher MRR and good dimensional accuracy were generated by $NaNO_3$ electrolyte mixed with additive chemicals [22]. Machining with higher concentration of electrolyte yields superior MRR [16]. Acid-based electrolytes and salt-based electrolytes are required to machine some unique materials [23–26]. μECM of stainless workpiece requires the mixture of 6 M (mole) HF and 3 M HCl electrolytes [27, 28]. The textured characteristic of micromachined samples was examined with hybrid electrolyte combination of NaCl and $NaNO_3$ [29].

Vertical cross-flow electrolyte delivery arrangement was utilized in μECM setup to fabricate micro-circular pattern [30]. Citric acid as electrolyte solution used to control the deposition rates during cleaning of the metal and metal deposition process [31]. The usage of citric acid as electrolyte solution in μECM process prevents the formation non-soluble agents on the outside of the electrode [32]. It is reported that the advisable citric acid level in μECM process is 0.3 M [12]. Some researchers proposed that hybrid combination of sodium chloride, sodium nitrate and citric acid can provide a better machining quality in μECM experimentations [33]. This experimental investigation attempts to analyze the performance of NaCl, $NaNO_3$ and hybrid combination of citric acid/NaCl/$NaNO_3$ as electrolyte solutions for micromachining Hastelloy C276 in electrochemical environment. Being non-passive electrolyte, NaCl is aggressive in nature. Hence, it enhances the anodic dissolution process. Therefore, MRR is increased and surface quality marginally affected while machining with NaCl electrolyte. $NaNO_3$ is a passive electrolyte. In comparison with NaCl, it produces less MRR, but surface quality gets improved. In hybrid electrolyte combination, NaCl helps to improve the MRR and $NaNO_3$ helps to improve the surface quality. Being natural electrolyte, citric acid tends to reduce the corrosion effect.

2.3 Electrode Selection

Electrode material is selected based on the following parameters: good heat and current conductivity and also it must withstand the pressure generated during electrolyte flushing. The preferred electrode materials are copper/copper alloys, platinum, tungsten, titanium and molybdenum. It is reported that selection of proper tool feed rate plays a key role in obtaining superior MRR and good surface finish. For better MRR and good machining accuracy, copper-based tools are always recommended [34, 35]. Hence, in this research work, copper-based brass electrode with a diameter of 400 μm is selected for the micromachining experiments.

2.4 Experimental Setup

Figure 1a represents the experimental arrangement of the electrochemical micromachining setup. The machining unit, electrode feeding assembly, electrolyte delivery unit and con-

Table 1 Chemical composition of Hastelloy C276 (wt%)

Ni	Cr	Mo	Fe	Mn	Co	C	P	W	S	V	Si
56.56	15.01	16.08	6.49	0.44	0.09	0.008	0.033	3.75	0.019	0.094	0.025

Table 2 Properties of Hastelloy C276

Melting point (°C)	Mass density (g/cm^3)	Ultimate tensile strength (MPa)	Hardness (HRB)	Modulus of elasticity (GPa)	Poisson's ratio
1350	8.89	792	90	410	0.31

Fig. 1 **a** ECMM setup, **b**, **c** sample specimens

trol system are the basic components of the µECM setup. The required amount of electrolyte solution with proper concentration is filled in the electrolyte chamber. The pump and filters are used for electrolyte filtration and re-circulation process. The level of electrolyte in the tank is maintained based on the workpiece and tool immersion depth. Fixture was designed to hold the workpiece with the dimensions of 40 mm × 10 mm (length × width) and immersed within the electrolyte chamber. Micromachined Hastelloy C276 samples are indicated in Fig. 1b, c.

2.5 Experimental Procedure

Hastelloy C276 with a dimension of $40 \times 10 \times 0.15$ mm is rigidly fixed on the work holding fixture of µECM machine. Electrolyte chamber is filled with adequate amount of selected electrolyte solutions. DC power supply with predefined T_{ON} and T_{OFF} time is applied during µECM process. MRR, surface roughness (Ra) and overcut are measured as output performances to analyze the processing nature of various electrolytes while machining Hastelloy C276. The chosen input parameters for the µECM process are operating voltage (V), concentration of electrolyte (COE); micro-tool feed rate (MTFR) and duty cycle (DC) [36]. The weights of the specimens are measured by a micro-weighing machine with an electronic balance setup. Micro-drilling was done for all the experiments and machining time was recorded using a stopwatch. By products of reactions are flushed out by the electrolyte which is fed at a rate of 1 m/s. The qualities of the micromachined surfaces were examined using a scanning electron microscope. The formulae given in Eqs. 1, 2, 3 and 4 are used to calculate MRR, circularity, conicity and overcut, respectively.

$$\text{REMOVAL RATE} = \frac{\text{Initial Weight of the Specimen} - \text{Final Weight of the Specimen}}{\text{Machining Time}} \quad (1)$$

$$\text{CIRCULARITY} = \text{Major Diameter} - \text{Minor Diameter} \quad (2)$$

$$\text{CONICITY} = \frac{\left(\frac{\text{Major Diameter at entry}+\text{Minor Diameter at entry}}{2}\right) - \left(\frac{\text{Major Diameter at exit}+\text{Minor Diameter at exit}}{2}\right)}{2 \times \text{Thickness of the specimen}} \quad (3)$$

$$\text{OVERCUT} = \left(\frac{\left(\frac{\text{Major axis}+\text{Minor axis}}{2}\right) - \text{Tool Diameter}}{2}\right). \quad (4)$$

2.6 Taguchi Design of Experiments

Taguchi approach is one of the best and effective tools for designing and conducting experiments. Using Taguchi method, better results can be obtained by carrying out least number of experiments. Equation 5 is applied to find the minimum number of experiments.

$$\text{DOF} = (A-1)(B) + (A-1)2(C) + 1 \quad \text{for the average,} \quad (5)$$

where DOF is the degree of freedom, B—number of independent variables, A—levels and C—number of interactions.

Table 3 μECM parameters and their levels

Factors	Level 1	Level 2	Level 3
Operating voltage (V)	8	10	12
Concentration of electrolyte (g/l)	20	25	30
Duty cycle (%)	33	50	66
Micro-tool feed rate (mm/min)	0.5	0.75	1

The minimum number of experiments to be carried out is greater than or equal to DOF. The chosen μECM factors and their levels are indicated in Table 3 [13].

3 Results and Discussion

The output responses of the μECM process were systematically investigated with respect to various machining factors. Tables 4, 5 and 6 illustrate the experimental results on micromachining of Hastelloy C276 using the μECM process as per L9 orthogonal array. The input parameters and the corresponding output performance measures are listed in these tables. The MRR, overcut, conicity and circularity values are calculated based on the formulae provided in Eqs. 1, 2, 3 and 4, respectively.

3.1 Impact of Electrolytes and Machining Factors on MRR

Figures 2 (bar chart) and 3 (main effect plot) display the effectiveness of electrolytes and machining factors on material removal rate during μECM process. From the bar chart, it is apparent that for most of the experimental conditions MRR is higher while machining with hybrid electrolyte. The maximum divergence from the mean line in main effect plot is the indication of very good machining conditions for superior MRR. Figure 3c shows the maximum deviation from the mean line which clearly proves that hybrid electrolyte is the most favorable electrolyte for machining Hastelloy C276 using μECM process followed by NaCl and $NaNO_3$. In hybrid electrolyte combination, citric acid acts as a catalyst during material removal process which enhances the MRR. Citric acid also controls the micromachining process which in turn produces less overcut and minimum conicity. Being non-passive in nature, NaCl is an aggressive electrolyte which produces higher MRR but at the same time it also causes high stray current effect due to which larger stray dissolution zone is observed. The passive $NaNO_3$ electrolyte produces lower MRR and minimum stray dissolution zone.

Operating voltage and duty cycle are the predominant machining variables affecting the MRR while micromachining with NaCl and hybrid electrolyte (Fig. 3a–c). According to Fig. 3b, it is validated that concentration of electrolyte is the key parameter which influences the MRR while machining with $NaNO_3$ electrolyte. The inter-electrode gap (IEG) was maintained less than 0.1 mm to minimize the nonlinearity effect produced by the polarization voltage in μECM process [37]. The maximum material was removed once the micro-spark has occurred during machining process. Occurrence of micro-spark causes the easy breaking of hydrogen bubbles at higher voltage. On a whole, the μECM characteristic indicates that superior MRR is produced while machining with hybrid electrolyte as compared to the other two electrolytes.

3.2 Effect of Electrolytes and Machining Factors on Overcut

Average overcut values calculated from each specimen are indicated in Fig. 4 as a bar chart. It is noticeable that each and every machining factor has an appreciable amount of influence on the overcut. For majority of experimental conditions, the overcut value is high while machining with NaCl electrolyte followed by $NaNO_3$ and hybrid electrolytes. The overcut on the machined surfaces is directly proportional to the input voltage, concentration of electrolyte and tool feed rate. Figure 5a–c illustrates the main effect plot for overcut values with respect to different types of electrolytes and process parameters used in this study. It is apparent from Fig. 5a that the electrode feed rate is the most predominant input factor which affects the overcut values while machining with NaCl electrolyte. The overcut value is appreciably depending on the concentration of electrolyte whenever $NaNO_3$ is used as an electrolyte (Fig. 5b). Figure 5c validates that the voltage and duty cycle have significant effect on overcut while machining with hybrid electrolyte. The hybrid electrolyte produces lower overcut in comparison NaCl and $NaNO_3$ electrolyte.

3.3 Impact of Electrolytes and Machining Factors on Circularity

Figures 6 and 7 illustrate the consequence of electrolytes and machining factors on circularity. Difference between major and minor diameter is the measure of circularity. In Fig. 7, the deviations from horizontal lines indicate the more influence of machining factors on output responses. It is also clear from Figs. 6 and 7 that most circular holes are produced while machining with hybrid electrolyte. All input variables are equally significant while machining with hybrid electrolyte. Duty cycle has most significant effects on circularity while machining with NaCl electrolyte. Concentration of electrolyte has most significant effects on circularity while machining with $NaNO_3$ electrolyte. From Fig. 7, it is inferred that hybrid electrolyte combinations produce most circular micro-holes.

Table 4 Orthogonal array L9 responses—machining with NaCl electrolyte

Exp. no.	Operating voltage (V)	Concentration of electrolyte (g/l)	Micro-tool feed rate (mm/min)	Duty cycle (%)	MRR (mm^3/min)	Overcut (µm)	Conicity (µm)	Circularity (µm)
1	8	20	0.5	33	0.041173	433.00	3.0000	141
2	8	25	0.75	50	0.031804	101.75	9.0000	427
3	8	30	1	66	0.034909	76.25	14.5000	243
4	10	20	0.75	66	0.058101	6.00	9.3333	427
5	10	25	1	33	0.030613	24.25	0.3333	164
6	10	30	0.5	50	0.081306	182.50	4.3333	443
7	12	20	1	50	0.066729	39.75	8.5000	405
8	12	25	0.5	66	0.147991	174.25	13.6000	413
9	12	30	0.75	33	0.039688	141.75	4.5000	179

Table 5 Orthogonal array L9 responses—machining with $NaNO_3$ electrolyte

Exp. no.	Operating voltage (V)	Concentration of electrolyte (g/l)	Micro-tool feed rate (mm/min)	Duty cycle (%)	MRR (mm^3/min)	Overcut (µm)	Conicity (µm)	Circularity (µm)
1	10	20	0.5	33	0.0166866	30.50	0.6666	126
2	10	25	0.75	50	0.0467544	63.00	1.5000	134
3	10	30	1	66	0.0523249	100.50	3.8300	144
4	12	20	0.75	66	0.0276926	29.00	0.6666	88
5	12	25	1	33	0.0424276	56.25	3.3330	137
6	12	30	0.5	50	0.0664327	164.50	6.6667	146
7	14	20	1	50	0.0252818	33.25	1.8333	109
8	14	25	0.5	66	0.0286457	67.75	2.3333	142
9	14	30	0.75	33	0.0437444	92.50	2.8889	134

Table 6 Orthogonal array L9 responses—machining with hybrid electrolyte

Exp. no.	Operating voltage (V)	Concentration of electrolyte (g/l)	Micro-tool feed rate (mm/min)	Duty cycle (%)	MRR (mm^3/min)	Overcut (µm)	Conicity (µm)	Circularity (µm)
1	8	25	0.5	33	1.09163	45.50	0.5556	164
2	8	30	0.75	50	0.84150	29.00	1.6667	152
3	8	35	1	66	0.01892	13.75	6.8333	237
4	10	25	0.75	66	0.01595	8.50	4.3333	406
5	10	30	1	33	1.12640	35.00	4.0000	174
6	10	35	0.5	50	0.11715	18.50	0.8333	302
7	12	25	1	50	0.02583	97.75	1.8333	126
8	12	30	0.5	66	0.01004	46.00	0.1666	427
9	12	35	0.75	33	0.04478	132.00	3.6667	408

3.4 Upshot of Electrolytes and Machining Factors on Conicity

Figures 8 and 9 demonstrate the influence of electrolytes and machining factors on conicity. The bar chart and main plot indicate that minimum conicity is observed while machining with hybrid electrolyte. Duty cycle has greater influence on conicity while machining with NaCl electrolyte and concentration of electrolyte has major effect on conicity while machining with $NaNO_3$ electrolyte.

Overall results indicate that the Hastelloy C276 machined by µECM process with hybrid electrolyte (mixture of NaCl, $NaNO_3$ and citric acid) produces maximum MRR, minimum overcut, good circular holes and minimal conicity. In hybrid

Fig. 2 Impact of electrolytes and machining factors on MRR

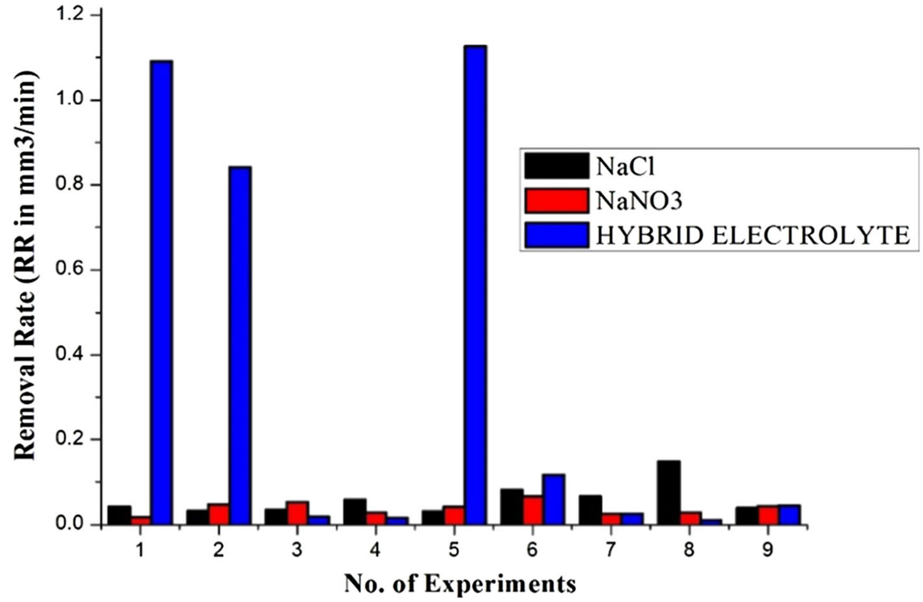

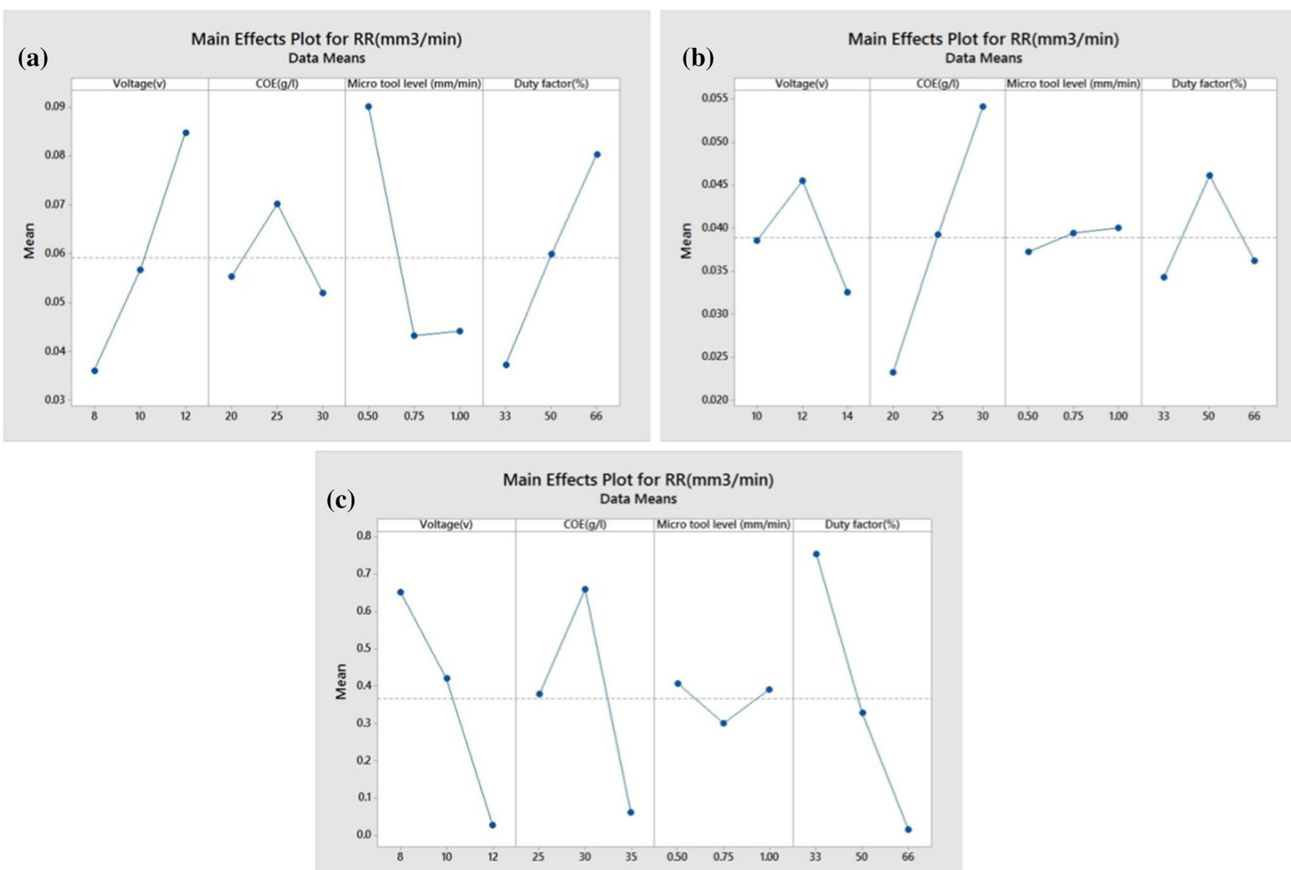

Fig. 3 Influence of process parameters on MRR while machining with **a** NaCl, **b** $NaNO_3$ and **c** hybrid electrolyte

electrolyte combination, due to aggressive nature, NaCl helps to produce maximum MRR, the passive nature of $NaNO_3$ helps to reduce the stray dissolution zone (SDZ) and citric acid acts as an additive agent to improve the overall machining performances.

Fig. 4 Influence of electrolytes and machining factors on overcut

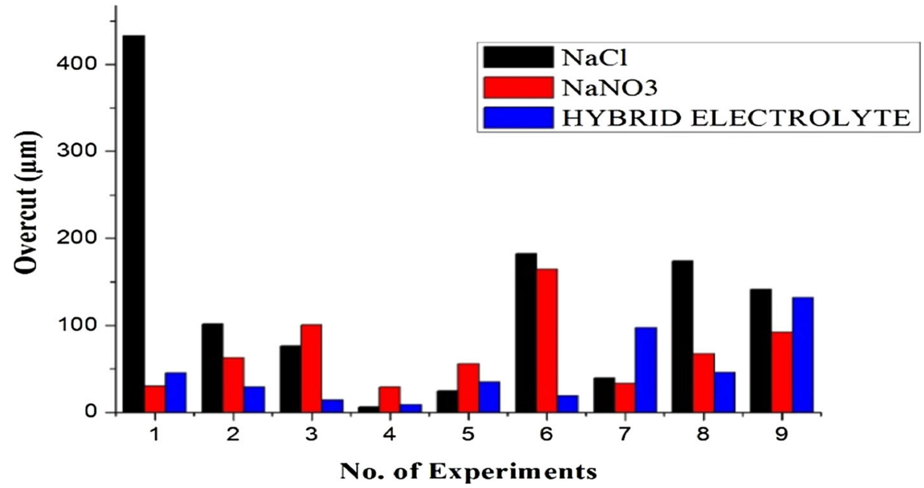

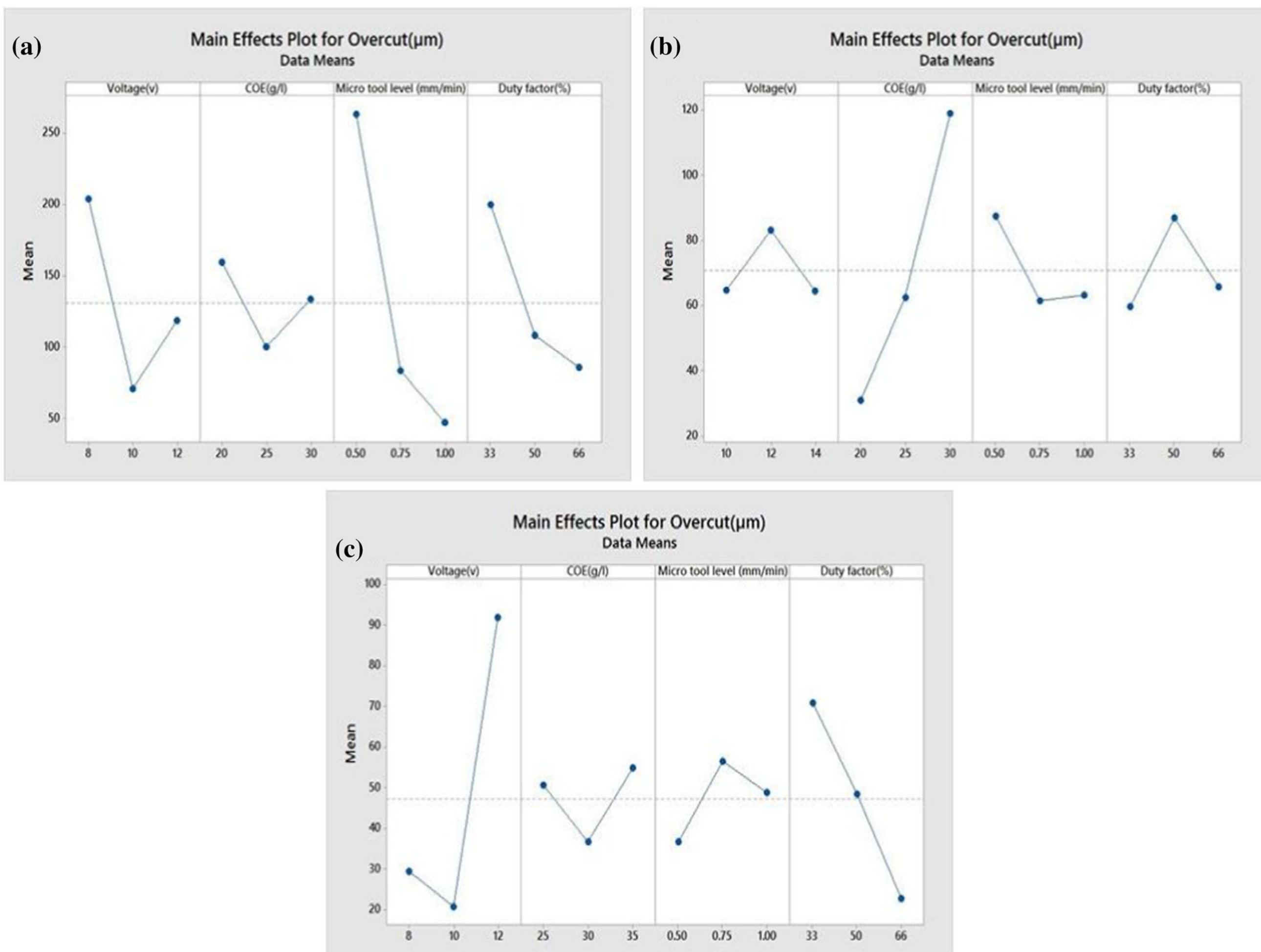

Fig. 5 Influence of process parameters on overcut while machining with **a** NaCl, **b** $NaNO_3$ and **c** hybrid electrolyte

3.5 Taguchi Approach

Taguchi technique is normally employed to mitigate the required number of experiments and also minimizes the processing variations. Signal/noise (*S*/*N*) ratio values were calculated to identify the best quality components. It is necessary to achieve maximum MRR, hence, consider the "larger-the- better" type of quality component [38]. The for-

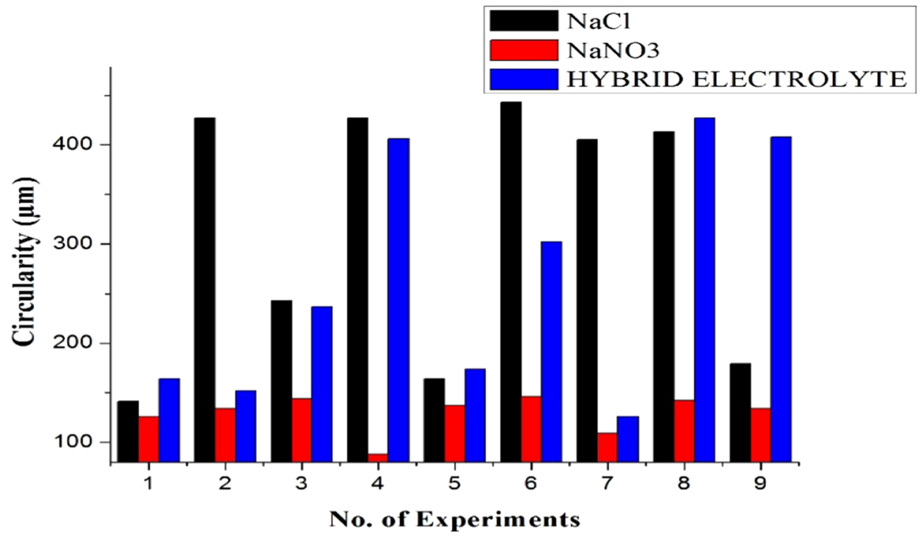

Fig. 6 Impact of electrolytes and machining factors on circularity

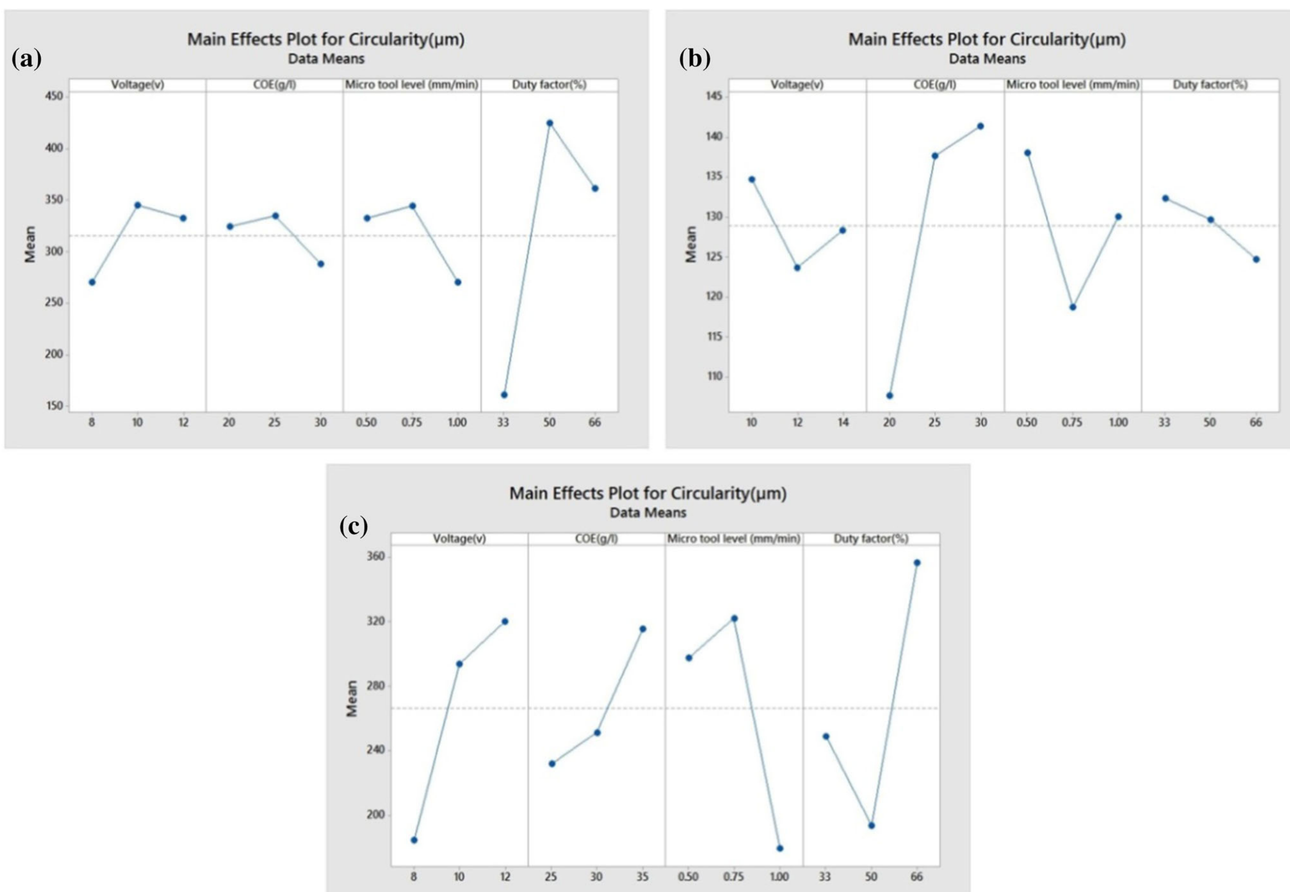

Fig. 7 Influence of machining factors on circularity while machining with **a** NaCl, **b** $NaNO_3$ and **c** hybrid electrolyte

mula provided in Eq. 6 is used to calculate the *S*/*N* ratio for MRR.

$$S/N\text{ ratio} = -10 * \log\left(\frac{1}{a}\right)\sum\left(\frac{1}{M_{jp}^{2}}\right). \quad (6)$$

Formula given in Eq. 7 is applied to determine the *S*/*N* ratios for circularity, conicity and overcut. These output performances are judged as better when their *S*/*N* ratio is lesser.

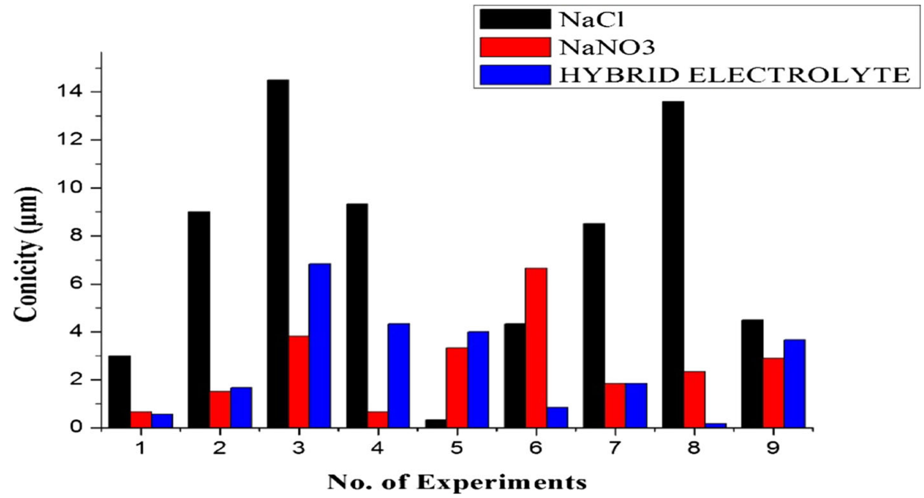

Fig. 8 Influence of electrolytes and machining factors on conicity

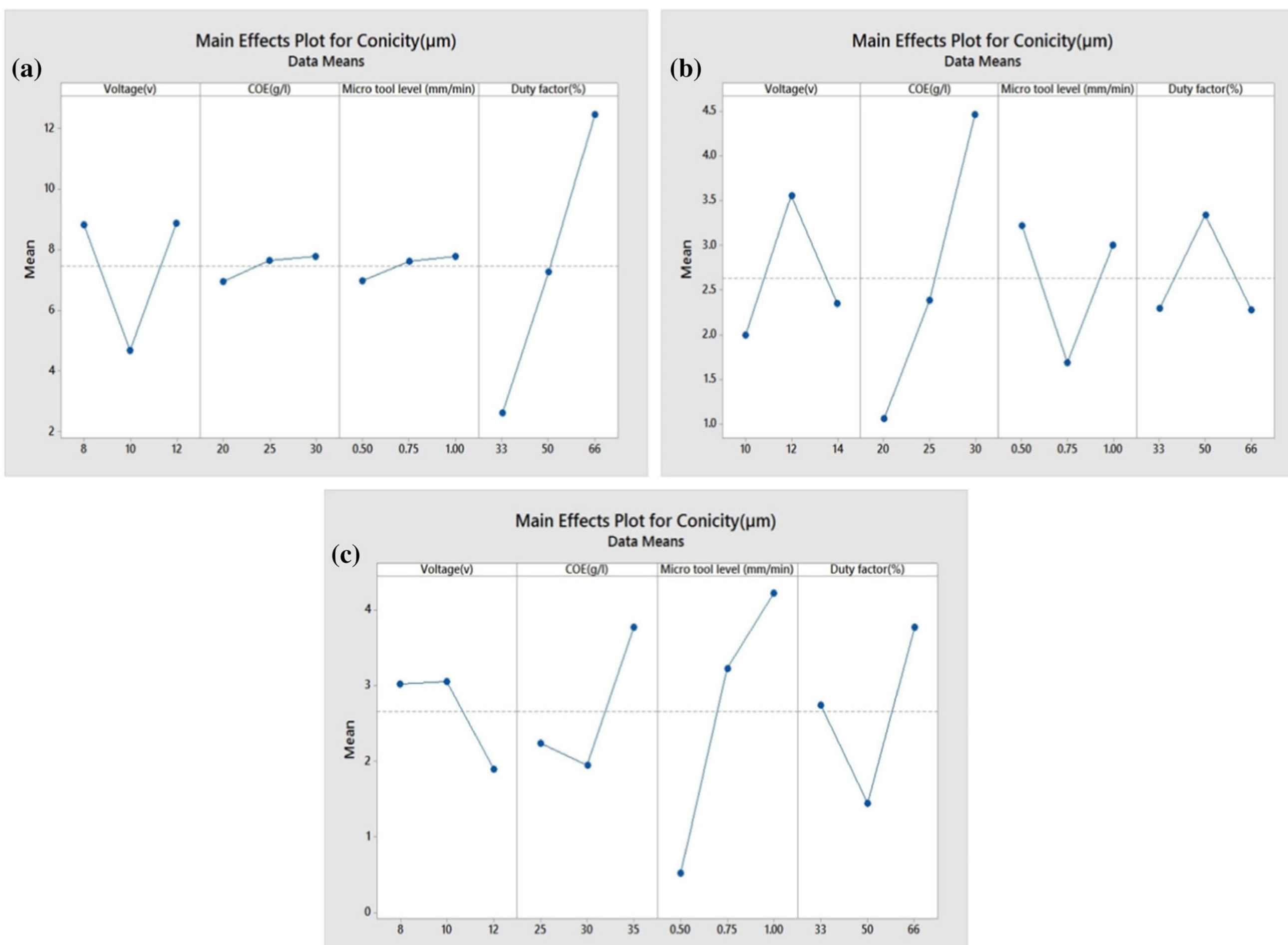

Fig. 9 Influence of machining factors on conicity while machining with **a** NaCl, **b** $NaNO_3$ and **c** hybrid electrolyte

In Eqs. 6 and 7, a—number of trials and M_{jp}—response of j_{th} experiment of p_{th} contingent level.

$$S/N\ \text{ratio} = -10 * \log\left(\frac{1}{a}\right)\sum M_{jp}^2. \tag{7}$$

Grey relational approach is exercised to test the multiple performances of the components and change the performance into distinct grey relational grade [39]. This process is done in three stages. According to Eqs. 8 and 9, the values of normalized S/N ratios are calculated. The Taguchi design

Table 7 *S/N* and normalized *S/N* values for the response of MRR

S. no.	Sodium chloride (NaCl)		Sodium nitrate ($NaNO_3$)		Hybrid electrolyte	
	MRR		MRR		MRR	
	W1	W2	W1	W2	W1	W2
1	– 33.90459023	0	– 35.55264289	0	0.761509247	0.993357341
2	– 29.9503651	0.438445169	– 26.60355024	0.747453159	– 1.718428292	0.932869847
3	– 29.14125184	0.275189604	– 25.62583186	0.829114923	– 34.46157736	0.134240455
4	– 24.71632785	0.530828186	– 31.15272535	0.367493376	– 35.94478625	0.098063903
5	– 30.28188427	0.419292625	– 27.44703069	0.677003342	1.033852836	1
6	– 42.79754809	0.699453167	– 23.57986233	1	– 18.62515414	0.541502418
7	– 23.51370767	0.600306469	– 31.94384017	0.301417261	– 31.75751188	0.410404593
8	– 16.5952939	1	– 30.85881142	0.394144003	– 39.96532574	0
9	– 28.02681572	0.339573279	– 27.18155072	0.699176948	– 26.97831843	0.316762627

W1—*S/N* value, W2—Normalized *S/N* value

analysis is being regulated between 0 and 1. In Eqs. 8 and 9, Q_{jp} is the normalized *S/N* value, S_{jp}—*S/N* value derived in Taguchi approach; min (S_{jp})—minimum *S/N* value and max (S_{jp})—maximum *S/N* value.

For "larger-the-better," normalized *S/N* value is determined by Eq. 8.

$$Q_{jp} = \left(\frac{S_{jp} - \min(S_{jp})}{(\max(S_{jp}) - \min(S_{jp}))}\right). \tag{8}$$

For "smaller-the-better," normalized *S/N* value is determined by Eq. 9.

$$Q_{jp} = \left(\frac{\max(S_{jp}) - S_{jp}}{\max(S_{jp}) - \min(S_{jp})}\right). \tag{9}$$

In stage 2, formula provided in Eq. 10 is utilized to find the grey relational coefficient (BD_{jp}). The optimization process includes both "larger-the-better" and "smaller-the-better," and hence, the value @ (differentiate coefficient) is taken as 0.5. The notations $\$_{min}$ and $\$_{max}$ indicate the least and highest deviation from the intended value. These values are considered as quality loss.

$$BD_{jp} = \left(\frac{\$_{min} + @\$_{max}}{\$_{jp} + @\$_{max}}\right). \tag{10}$$

Equation 11 is employed to find the grey relational grade (B_j), where "*a*" indicates the amount of responses. Good response in a machining process is also known as ideal sequence. Superior relational grade between ideal and present sequence specify the most favorable responses [40, 41].

$$B_j = \left(\frac{1}{a}\right) \sum BD_{jp}. \tag{11}$$

The *S/N* and the normalized *S/N* values for MRR, overcut, conicity and circularity are represented in Tables 7, 8, 9 and 10, respectively. The calculation is done in such a way that the superior *S/N* value is better for MRR and the lower *S/N* value is better for overcut, conicity and circularity. Table 7 reveals that the *S/N* value and normalized *S/N* value is higher for the experiment 8 whenever NaCl electrolyte is used. For $NaNO_3$ and hybrid electrolytes, experiments 6 and 5 provide the better results.

Tables 11, 12 and 13 represent the grey relational coefficient and converted grey relational grades. All the experiments are carried out by using the differentiate coefficient value of 0.5 [42]. The better machining parameters are identified by the higher grey grade, i.e., 8th, 6th and 5th experiments for NaCl, $NaNO_3$ and hybrid electrolyte in Tables 11, 12 and 13, respectively. The average grey relational grade for machining variable is depicted in Table 14. The best value for each machining variable in a process is identified by its average value of grey relational level [43]. It is noted from Table 14 that the duty cycle is the most dominant parameter while machining with NaCl and hybrid electrolyte; whereas concentration of electrolyte is the most influencing parameter while machining with $NaNO_3$ electrolyte. The influence of the machining variables on determining the output responses is indicated by the max–min level in Table 14.

3.6 Confirmation Tests

Confirmation tests were performed to validate the integrity of the results obtained for the optimized output values. For NaCl electrolyte with respect to Table 11, experiment 8 gives the maximum GRG values (rank 1). Hence, the confirmation experiment was conducted with respect to the following parametric conditions: voltage—12 V, concentration of electrolyte—25 g/l, micro-tool feed rate—0.5 mm/min, duty cycle—66%. The following results are obtained from

Table 8 *S/N* and normalized *S/N* values for the response of overcut

S. no.	Sodium chloride (NaCl)		Sodium nitrate ($NaNO_3$)		Hybrid electrolyte	
	Overcut		Overcut		Overcut	
	W1	W2	W1	W2	W1	W2
1	− 46.96609726	1	− 29.68599679	0.029056479	− 33.16043793	0.611668899
2	− 40.15068836	0.782969996	− 35.98681099	0.447011009	− 29.24795996	0.447447284
3	− 37.64479696	0.703172345	− 40.04334434	0.716093401	− 43.76605396	0.175362377
4	− 15.56302501	0	− 29.24795996	0	− 18.58837851	0
5	− 27.69423486	0.386306466	− 35.00245054	0.381715017	− 30.88136089	0.516011028
6	− 45.43525738	0.944564663	− 44.32331805	1	− 25.34343457	0.283550673
7	− 31.98674266	0.543997162	− 30.43583299	0.078795676	− 39.80233532	0.890478431
8	− 44.82345574	0.931769685	− 36.61818599	0.48889437	− 33.25515663	0.615653633
9	− 41.63774279	0.830323784	− 39.34383465	0.668300855	− 42.41147862	1

W1—*S/N* value, W2—Normalized *S/N* value

Table 9 *S/N* and normalized *S/N* values for the response of conicity

S. no.	Sodium chloride (NaCl)		Sodium nitrate ($NaNO_3$)		Hybrid electrolyte	
	Conicity		Conicity		Conicity	
	W1	W2	W1	W2	W1	W2
1	− 9.542425094	0.582402748	3.543693814	0	5.104755259	0.32430358
2	− 40.08485040	0.873590869	− 3.542825181	0.352419888	− 4.437148708	0.641093018
3	− 23.43736004	1	− 11.66397548	0.759298838	− 16.69260976	1
4	− 40.40070451	0.883439408	3.543693814	0	− 12.73637514	0.877360701
5	9.543293727	0	− 10.45670627	0.698938131	− 12.04140983	0.855810964
6	− 12.73637514	0.679866475	− 16.47842825	1	1.583972363	0.433444313
7	− 18.58837851	0.858440983	− 5.264670769	0.439348403	− 5.264670769	0.645745371
8	− 43.67077817	0.983015845	− 7.359411642	0.54408046	15.56650006	0
9	− 13.06425028	0.68987162	− 9.424650178	0.636838158	− 11.28550757	0.832385264

W1—*S/N* value, W2—Normalized *S/N* value

Table 10 *S/N* and normalized *S/N* values for the response of circularity

S. no.	Sodium chloride (NaCl)		Sodium nitrate ($NaNO_3$)		Hybrid electrolyte	
	Circularity		Circularity		Circularity	
	W1	W2	W1	W2	W1	W2
1	− 41.58362492	0	− 42.0074109	0.708999603	− 44.29687696	0.301534056
2	− 46.72940468	0.839613167	− 42.54419597	0.830590683	− 43.63687176	0.424608092
3	− 47.71443547	1	− 43.16724984	0.972754997	− 47.49496692	0.743738395
4	− 46.72940468	0.839613167	− 38.88965344	0	− 45.84514243	0.505445546
5	− 44.29687696	0.442726898	− 42.73441134	0.874324529	− 44.81098497	0.369244635
6	− 46.52671743	0.806574505	− 43.28705712	1	− 49.60013886	1
7	− 45.80069433	0.688107540	− 40.74852996	0.443742372	− 42.0074109	0
8	− 46.14994176	0.745091854	− 41.65570741	0.629040796	− 46.72940468	0.642882386
9	− 45.05706062	0.566767625	− 42.54419597	0.830590683	− 45.93330381	0.517059603

W1—*S/N* value, W2—Normalized *S/N* value

Table 11 Grey relational coefficients—grade and rank while machining with NaCl

S. no.	Grey relational coefficient				Grey relational grade	Rank
	MRR	Overcut	Conicity	Circularity		
1	0.333333333	1	0.544901371	0.333333333	0.552894109	8
2	0.393240378	0.697341889	0.79841037	0.757134095	0.661468158	4
3	0.40843645	0.627488261	1	1	0.758928678	2
4	0.515904397	0.333333333	0.810673914	0.757134095	0.60426091	6
5	0.387384476	0.448956544	0.333333333	0.472914708	0.410647265	9
6	0.624573079	0.900404797	0.609656824	0.742057999	0.713870675	3
7	0.555744798	0.51176924	0.779351528	0.615845092	0.615677665	5
8	1	0.879924894	0.967147629	0.662334336	0.87735140	1
9	0.430875979	0.746629473	0.61718613	0.53577434	0.582615956	7

Table 12 Grey relational coefficients—grade and rank while machining with $NaNO_3$

S. no.	Grey relational coefficient				Grey relational grade	Rank
	MRR	Overcut	Conicity	Circularity		
1	0.333333333	0.339917878	0.333333333	0.634210934	0.40967387	8
2	0.66441047	0.474838773	0.435640714	0.74692716	0.580449029	5
3	0.745284128	0.637830918	0.675036068	0.948325725	0.75164042	2
4	0.441498542	0.333333333	0.333333333	0.333333333	0.36037463	9
5	0.607535866	0.44711343	0.624171514	0.799136331	0.640489233	4
6	1	1	1	1	1	1
7	0.417159353	0.351814297	0.471408239	0.464132479	0.426128592	7
8	0.451280605	0.494507148	0.523056574	0.57406586	0.510727547	6
9	0.624357652	0.601178927	0.579265643	0.74692716	0.637932346	3

Table 13 Grey relational coefficients—grade and rank while machining with hybrid electrolyte

S. no.	Grey relational coefficient				Grey relational grade	Rank
	MRR	Overcut	Conicity	Circularity		
1	0.986888867	0.562853407	0.425279852	0.417410007	0.598055481	3
2	0.88163184	0.47503559	0.568241883	0.388986423	0.578473934	6
3	0.366096654	0.377461723	1	0.643284059	0.596710609	5
4	0.356649637	0.333333333	0.803033154	0.502737681	0.498938451	8
5	1	0.508135776	0.776169684	0.444284393	0.681624038	1
6	0.510465783	0.411032329	0.468798775	1	0.597574432	4
7	0.384672965	0.841315516	0.585305579	0.333333333	0.530906848	7
8	0.333333333	0.56538933	0.333333333	0.569399807	0.450363951	9
9	0.443569479	1	0.748934936	0.508677842	0.670045564	2

the confirmation test: MRR—0.142823 mm^3/min, overcut—170.224825 µm, conicity—13.09408 µm and circularity—403.7488 µm. The calculated error percentage for MRR is 3.49%, overcut is 2.31%, conicity is 3.72%, and circularity is 2.24%.

Similarly for $NaNO_3$ electrolyte, experiment 6 provides rank 1 (Table 12) and the corresponding parametric conditions are as follows: voltage—12 V, concentration of electrolyte—30 g/l, micro-tool feed rate—0.5 mm/min and duty cycle—50%. The output values obtained through the confirmation test are MRR—0.63330292 mm^3/min, overcut—33.6035 µm, conicity—3.8704 µm and circularity—169.9458 µm. The error percentage found by comparing the confirmation test and experimentation values is as follows: MRR error%—4.67%, overcut error%—4.38%, conicity error% 2.90% and circularity error%—3.12%.

Experimental condition 5 yields (Table 13) the maximum GRG value for hybrid electrolyte and the corresponding machining conditions are as follows: voltage—10 V, concentration of electrolyte—30 g/l, micro-tool

Table 14 Average grey relational grade for each machining variable

Factor notation	Average grey relational grade									Max.–min.		
	Sodium chloride (NaCl)			Sodium nitrate ($NaNO_3$)			Hybrid electrolyte			NaCl	$NaNO_3$	Hybrid electrolyte
	Level 1	Level 2	Level 3	Level 1	Level 2	Level 3	Level 1	Level 2	Level 3			
Operating voltage	0.6577	0.5762	0.6918	0.5805	0.6599	0.5249	0.5910	0.5927	0.5504	0.1156	0.1350	0.0443
Concentration of electrolyte	0.5909	0.6498	0.6851	0.3987	0.5704	0.7965	0.5426	0.5701	0.6424	0.0944	0.3977	0.0788
Micro-tool feed rate	0.7147	0.6161	0.5950	0.6401	0.5262	0.5990	0.5486	0.5824	0.6030	0.1406	0.1138	0.0544
Duty Cycle	0.5153	0.6636	0.7468	0.5556	0.6688	0.5409	0.6499	0.5689	0.5153	0.2314	0.1279	0.1345

Average grey relational grade while machining with NaCl = 0.641968; Average grey relational grade while machining with $NaNO_3$ = 0.590824; Average grey relational grade while machining with hybrid electrolyte = 0.578077

feed rate—1 mm/min, duty cycle—33%. Based on the confirmation test, the following output values are calculated. MRR—1.09463552 mm^3/min, overcut—33.6035 µm, conicity—3.8704 µm and circularity—169.9458 µm. The calculated error percentage is as follows: MRR—2.82%, overcut—3.99%, conicity—3.24%, circularity—2.33%.

3.7 Morphology of Micromachined Surfaces

To identify the kind of morphology of micromachined surfaces, scanning electron microscopy (SEM) micrographs were taken on the micromachined samples. Three samples were considered from each set of experiments. Samples are chosen based on the better machining quality; moderate machining quality and poor machining quality. The corresponding SEM micrographs are illustrated in Fig. 10.

Figure 10a represents the entry side SEM picture of a micro-hole cut on Hastelloy C276 by utilizing NaCl as electrolyte solution. The micro-hole is almost circular in nature with minimum conicity and overcut. Very small amount of stray dissolution zone (SDZ) is seen in the picture. The irregularities observed on the surface are also very marginal. The following parametric conditions are related to this experiment: operating voltage 8 V, concentration of electrolyte 20 g/l, micro-tool feed rate 0.5 mm/min and duty cycle 33%. In these parametric conditions, the flushing time is comparatively higher; hence, higher reaction byproducts are produced. Figure 10d represents the moderate machining quality obtained while machining with NaCl electrolyte. This is observed with the following machining conditions: operating voltage 10 V, concentration of electrolyte 30 g/l, micro-tool feed rate 0.5 mm/min and duty cycle 50%. In this experiment, T_{ON} and T_{OFF} time is equal, which influences moderate machining quality. The poor machined surface is observed while machining under the following parametric conditions, i.e., operating voltage 10 V, concentration of electrolyte 20 g/l, micro-tool feed rate of 0.5 mm/min and duty cycle 33% (Fig. 10g). Due to low electrode feed rate, large stray dissolution zone and white patches are formed in the workpiece.

While machining the Hastelloy C276 specimens by $NaNO_3$ electrolyte, the better micro-hole quality is achieved with the following machining conditions: operating voltage 12 V, concentration of electrolyte 30 g/l, electrode feed rate 0.5 mm/min and duty cycle 50% (Fig. 10b). When the machining is done with the high operating voltage and high concentration of electrolyte, good material removal is observed with better accuracy. The moderate quality of micro-hole is observed in Fig. 10e under the following parametric conditions, i.e., operating voltage 10 V, concentration of electrolyte 25 g/l, micro-tool feed rate 0.75 mm/min and duty cycle 50%. Low stray current effect and irregular circularity are observed. Figure 10h indicates the poorly machined

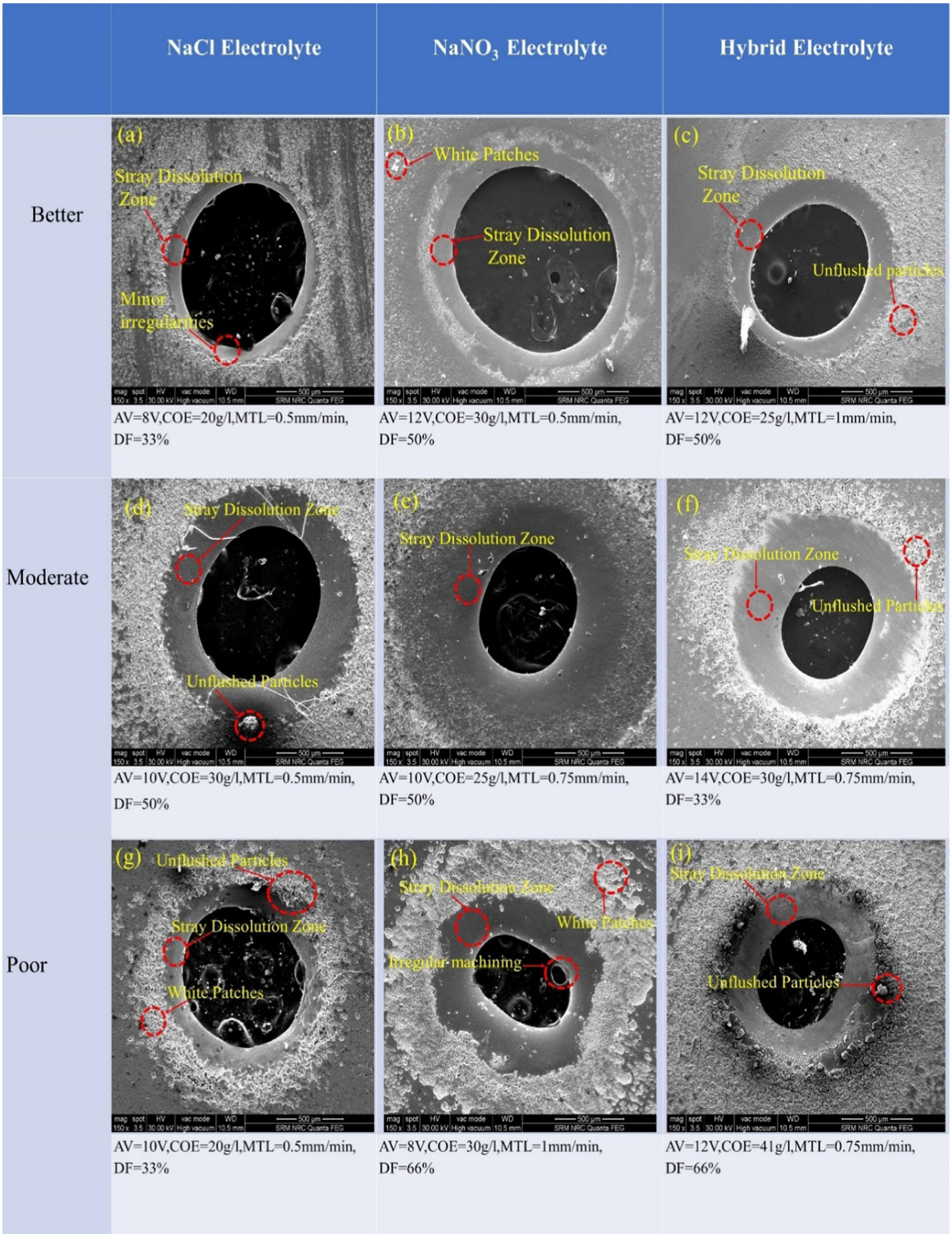

Fig. 10 SEM micrographs of micromachined Hastelloy C276 surfaces: **a**, **d**, **g** machined with NaCl electrolyte, **b**, **e**, **h** machined $NaNO_3$ electrolyte and **c**, **f**, **i** machined hybrid electrolyte

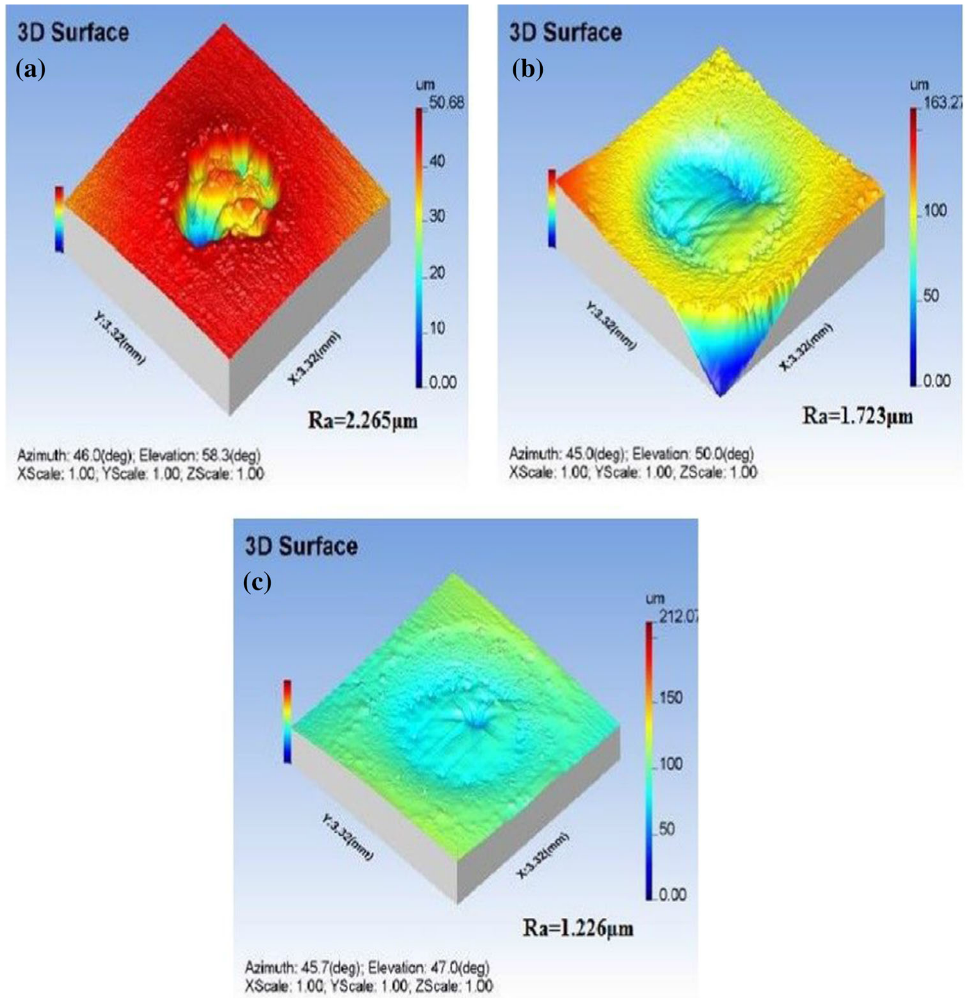

Fig. 11 3D surface roughness measurement of micromachined samples using **a** NaCl, **b** $NaNO_3$ and **c** hybrid electrolytes

micro-hole surface in Hastelloy C276 while machining with $NaNO_3$ electrolyte. This happened with the following machining conditions: operating voltage 8 V, concentration of electrolyte 30 g/l, micro-tool feed rate 1 mm/min and duty cycle 66%. In this condition, the material removed is less and the stray current effect is high because of the T_{ON} and T_{OFF} time ratio of 2:1. The increases in irregularities observed in the machined surfaces are due to the short time span of pulse off time. Less T_{OFF} time leads to improper removal of materials from the machined specimens.

When the micro-hole making is done with hybrid electrolyte (a combination of three individual electrolytes), the better micro-hole quality (Fig. 10c) is observed in the following parametric conditions: operating voltage 10 V, concentration of electrolyte 30 g/l, electrode feed rate 1 mm/min and duty cycle 33%. The T_{ON} and T_{OFF} time ratio is 1:2. As the T_{OFF} time is higher, machined products are removed properly, thus a better machined surface was achieved. The moderate micro-hole quality while machining with hybrid electrolyte is shown in Fig. 10f. The moderate results were observed in the following parametric conditions: operating voltage 12 V, concentration of electrolyte 35 g/l, micro-tool feed rate 0.75 mm/min and duty cycle 33%. Due to the maximum value of operating voltage and concentration of electrolyte with a moderate feed rate, the larger MRR happened in the stray current region than the actual machining zone. Hence, it is validated from Fig. 10f that the shape of the micro-hole is irregular. The machining conditions that produce poorly finished micro-hole (Fig. 10i) while machining with hybrid electrolyte are as follows: operating voltage 12 V, concentration of electrolyte 30 g/l, micro-tool feed rate 0.5 mm/min and duty cycle 66%.

3.8 Surface Roughness of the Micromachined Surfaces

TALYSURF CCI LITE non-contact 3D surface measurement device was employed to analyze the irregularities available on the surface of the micromachined holes. 3D surface roughness tester uses confocal and electron microscopy principle to measure the roughness values. The adjoining area immediately next to the produced micro-hole was considered for surface roughness measurement. Figure 11a shows the 3D surface measurement of surface roughness value of micro-machined Hastelloy C276 specimen which was machined using NaCl electrolyte. The average surface roughness (Ra) measured is approximately equal to 2.265 μm. This high value is due to the aggressive nature of NaCl electrolyte. It is noted in Fig. 11b that the average surface roughness value attained while machining with $NaNO_3$ electrolyte is around 1.723 μm. $NaNO_3$ electrolyte forms the submissive coat on the machined surface of the workpiece which minimizes the stray current effect and produces comparatively minimum surface roughness than NaCl. The average surface roughness observed while machining with hybrid electrolyte is 1.226 μm (Fig. 11c). Hybrid electrolyte has the combined property of aggressiveness of NaCl, passiveness of $NaNO_3$ and controlled machining of citric acid which in turn produces high MRR, low stray current effect and good surface finish.

4 Conclusions

Micro-hole making on Hastelloy C276 was carried out by micro-electrochemical machining process with NaCl, $NaNO_3$ and hybrid mixture (NaCl + $NaNO_3$ + citric acid) as electrolyte solutions. L9 orthogonal array and Taguchi grey relational approach were attempted to identify the optimized machining conditions. The prominent inferences arrived from the experiment and test results are presented below.

(i) Hybrid electrolytic combinations produced better material removal rate, lower overcut, lower conicity and most circular holes.

(ii) Taguchi grey relational approach reveals that the optimal parameters while machining with NaCl, $NaNO_3$ and hybrid electrolyte are as follows; for NaCl: operating voltage 12 V, concentration of electrolyte 25 g/l, electrode feed rate 0.5 mm/min and duty cycle 66%. Similarly, for $NaNO_3$: operating voltage = 12 V, concentration of electrolyte = 30 g/l, electrode feed rate = 0.5 mm/min and duty cycle = 50% and for hybrid electrolyte: operating voltage = 10 V, concentration of electrolyte = 30 g/l, electrode feed rate = 1 mm/min and duty cycle = 33%. Duty cycle is the most dominant factor while machining with NaCl and hybrid electrolyte and concentration of electrolyte is the most significant factor while machining $NaNO_3$ electrolyte.

(iii) Scanning electron microscopy pictures confirm that more surface irregularities and white patches are observed while machining with low micro-tool feed rate and high duty cycle.

(iv) The average surface roughness measured (1.226 μm) was lowest while machining with hybrid electrolyte. This value is 84% lesser than the average surface roughness produced while machining with NaCl electrolyte and 40% lower than the average surface roughness produced while machining with $NaNO_3$ electrolyte.

References

1. Yadav, A.K.: A review on research trend in corrosion resistant alloy (Hastelloy). Int. J. Inn. Res. In. Sci. Eng. **2**, 310–321 (2016)
2. Ezugwu, E.O.; Bonney, J.; Yamane, Y.: An overview of the machinability of aero engine alloy. J. Mater. Process. Technol. **134**, 233–253 (2003)
3. Ezugwu, E.O.; Wang, Z.M.; Okeke, C.I.: Tool life and surface integrity when machining Inconel 718 with PVD and CVD coated tools. Tri. Trans. **42**, 353–360 (2008)
4. Arunachalam, R.; Mannan, M.A.: Machinability of nickel based high temperature alloys. Mach. Sci. Technol. **4**, 127–168 (2000)
5. Choudhury, I.A.; Ei-Baradie, M.A.: Machining of nickel base super alloys Inconel 718. J. Eng. Manuf. **212**(3), 142–148 (1996)
6. Kitagawa, T.; Kubo, A.; Maekawa, K.: Temperature and wear of cutting tools in high speed machining of Inconel 718 and Ti-6Al-6V-2Sn. Wear **202**, 142–148 (1996)
7. Ezugwu, E.A.; Achado, A.R.; Rashloy, I.R.; Wallbank, J.: The effect of high-pressure coolant supply when machining a heat resistant nickel based super alloy. Lub. Eng. **47**, 751–757 (1991)
8. Uhlmann, E.; Mullany, B.; Biermann, D.; Rajurkar, K.P.; Hausotte, T.; Brinkomeier, E.: Process chains for high precision components with micro scale features. CIRP. Ann. Manuf. Technol. **65**, 549–572 (2016)
9. Masuzawa, T.: State of the art of micromachining. CIRP. Ann. Manuf. Technol. **49**, 473–488 (2000)
10. Imran, M.; Mativenga, P.T.; Gholinia, A.; Withen, P.J.: Evaluation of surface integrity in micro drilling process for nickel-based super alloy. Int. J. Adv. Manuf. Technol. **55**, 465–476 (2011)
11. Muthuramalingam, T.; Mohan, B.: A review on influence of electrical process parameters in EDM process. Arch. Civ. Mech. Eng. **15**, 87–94 (2015)
12. Ryu, S.H.: micro fabrication by electrochemical process in citric acid electrolyte. J. Mater. Process. Technol. **209**, 2831–2837 (2009)
13. Se, H.A.; Shi, M.R.; Deox, K.C.B.; et al.: Electrochemical micro drilling using ultra short pulses. Precis. Eng. **28**, 129–134 (2004)
14. Kim, B.H.; Ryu, S.H.; Choi, D.K.; et al.: Micro electrochemical milling. J. Micromech. MicroEng. **15**, 124 (2004)
15. Hen, W.; Kunieda, M.: A novel method to switch machining mode between micro-ECM and micro-EDM using oxide film on surface of tungsten electrode. Precis. Eng. **56**, 455–465 (2016)
16. Bhattacharyya, B.; Malapati, M.; Munda, J.; et al.: Influence of tool vibration on machining performance in electrochemical micro machining of copper. Int. J. Mach. Tool. Manuf. **47**, 335–342 (2007)
17. Lu, J.; Chai, E.S.; Zhou, H.D.: Physical properties of Hastelloy C276 at cryogenic temperatures. J. Appl. Phys. **103**(1–6), 064908 (2008)
18. Neergat, M.; Weibrod, K.R.: Electro dissolution of 304 stainless steel in neutral electrolytes for surface decontamination applications. Corros. Sci. **53**, 3983–3990 (2011)
19. Bhattacharyya, B.; Malapati, M.; Munda, J.: Experimental study on electrochemical micromachining. J. Mater. Process. Technol. **169**, 485–492 (2005)

20. Huaiquian, B.; Jiawen, X.; Ying, L.: Aviation-oriented micromachining technology micro ECM in pure water. Chin. J. Aeronaut. **21**, 455–461 (2008)
21. Yang, Y.; Natsu, W.; Zhao, W.: Realization of eco-friendly electrochemical micromachining using mineral water as an electrolyte. Precis. Eng. **35**, 204–213 (2011)
22. Thanigaivelan, R.; Arunachalam, R.M.; Kaethjpeyan, B.; Loganathan, P.: Electrochemical micro machining of stainless steel with acidified sodium nitrate electrolyte. In: The Seventeenth CIRP Conference of Electro Physical and Chemical Machining, Procedia CIRP **6**,351–355 (2013)
23. Trimmer, A.L.; Hudson, J.L.; Kock, M.; Schuster, R.: Single step electrochemical machining of complex nano structures with ultrashort voltage pulses. Appl. Phys. Lett. **82**, 3327–3329 (2003)
24. Landolt, D.; Chauuy, P.F.; Zinger, O.: Electrochemical micromachining, polishing and surface of metals: fundamentals aspects and new developments. Electr. Chem. Acta **48**, 3185–3201 (2003)
25. Kim, B.; Na, C.; Lee, Y.; et al.: Micro electrochemical machining of 3d micro structure using dilute sulfuric acid. CIRP. Ann. Manuf. Technol. **54**, 191–194 (2005)
26. Kim, B.H.; Ryu, S.H.; Choi, D.K.; Chu, C.N.: Microelectrochemical milling. J. Micromech. Microeng. **15**, 124–129 (2005)
27. Lee, E.S.; Baek, S.Y.; Cho, C.R.: A study of the characteristics for electrochemical micromachining with ultrashort voltage pulses. Int. J. Adv. Manuf. Technol. **31**, 762–769 (2007)
28. Cagnon, L.; Kirchner, V.; Kock, M.; et al.: Electro chemical micromachining of stainless steel by ultrashort voltage pulses. Z. Phys. Chem. **217**, 299–313 (2003)
29. Kirchner, V.; Cangnon, L.; Schuster, R.: Electrochemical machining of stainless steel microelements with ultrashort voltage pulses. Appl. Phys. Lett. **79**, 1721–1723 (2001)
30. Kumar, S.; Mahata, S.; Bhattacharyya, B.: Influence of electrolytes on surface texture characteristics generated by electrochemical micromachining. J. Micromanuf. **1**, 124–133 (2018)
31. Zerfaoui, M.; Oudda, H.; Hammouti, B.; Kertit, S.; Bekaddour, M.: Inhibition of corrosion of iron in citric acid media by amino acids. Prog. Org. Coat. **51**, 134–138 (2004)
32. Trettenhahn, G.; Koberi, A.: Anodic decomposition of citric acid on gold and stainless steel electrodes: an in situ-FITR-spectroscopic investigation. Electr. Chim. Acta **52**, 2716–2743 (2007)
33. Bhattacharyya, B.; Doloi, B.; Sridhar, P.S.: Electrochemical micro machining: new possibilities for micro-manufacturing. J. Mater. Process. Technol. **113**, 301–305 (2001)
34. Gangasagar, S.C.; Jayswal, M.T.: Effect of different electrodes and process variables on materials removal rate and surface roughness in electrochemical machining. Int. J. Adv. Eng. Sci. **1**, 19–24 (2011)
35. Sudjarso, A.; Ramdhani, N.L.; et al.: Material removal rate on electrochemical machining of brass, stainless steel and aluminium using brass electrodes. Int. J. Min. Metall. Mech. Eng. **1**, 15–17 (2013)
36. Sudiarso, A.; Ramdhani, N.L.F.; et al.: Overcut on electrochemical micromachining of brass, stainless steel and aluminium using brass electrodes. Int. J. Min. Metall. Mech. Eng. **1**, 10–13 (2013)
37. Bhattacharayya, B.; Munda, J.: Experimental investigation into electrochemical process. J. Mater. Process. Technol. **140**, 287–291 (2003)
38. Muthuramalingama, T.; Mohan, B.: Application of Taguchi-grey multi responses optimization on process parameters in electro erosion. Measurement **58**, 495–502 (2014)
39. Pradeep, N., Shanmuga Sundaram, K., Pradeep Kumar, M.: Multi-Response optimization of electro chemical micromachining parameter for SS304 using polymer graphite electrode with $NaNO_3$ electrolyte based on TOPSIS technique. J. Braz. Soc. Mech. Sci. Eng **41**, 323 (2019)
40. Antil, P.; Singh, S.; Manna, A.: Electrochemical discharge drilling of SiC reinforced polymer matrix composite using Taguchi's Gray relational Analysis. Arab. J. Sci. Eng. **43**, 1257–1266 (2018)
41. Muthuramalingama, T.; Mohan, B.: Taguchi-grey relational based multi response optimization of electrical process parameters in electrical discharge machining. Ind. J. Eng. Mater. Sci. **41**, 471–475 (2013)
42. Jailani, H.S.; Rajadurai, A.; Mohan, B.; et al.: Multi response optimization of sintering parameters of Al–Si alloy/fly ash composite using Taguchi method and grey relational analysis. Int. J. Adv. Manuf. Technol. **45**, 362–369 (2009)
43. Somashekhar, K.P.; Ramachandran, N.; Mathew, J.: Optimization of material removal rate in micro-EDM using artificial neural network and genetic algorithms. Mater. Manuf. Process. **25**, 467–475 (2010)